Journal of Research in Forestry, Wildlife & Environment Vol. 12(4) December, 2020
E-mail: jrfwe2019@gmail.com; jfewr@yahoo.com
http://www.ajol.info/index.php/jrfwe
jfewr ©2020 - jfewr Publications
ISBN: 2141 – 1778
Aigbokhan et al., 2020



# FOREST CANOPY DENSITY ANALYSIS OF SOKPOMBA FOREST RESERVE, EDO STATE

**Aigbokhan O. J [*] Pelemo O. J, Agbor C. F and Adamu I. S**

Department of Environmental Modeling and Biometrics, Forestry Research Institute of Nigeria
*Corresponding Author: *oseyomon255@gmail,com;* +234 805 403 9119

## ABSTRACT

***Forest is a dynamic landscape especially in the tropics as a result of high anthropogenic activities. This study therefore, attempts to evaluate the changes in forest canopy density sequel to the interaction between man and forest ecosystem in Sokpomba Forest Reserve from 1990 to 2020. Relevant Remote Sensing and GIS algorithms were used at different levels of this study. Landsat images formed the major input data for the analysis. In addition to the satellite images, ground control points (GCP) picked with the aid of Global Positioning System (GPS) were used to calculate the accuracy assessment of the Forest Canopy Density (FCD) analysis. The high canopy density (HD) decreased from 320.82km$^2$ in 1990 to 292.82km$^2$ in 2020. Conversely, the low canopy density (LD) increased from 171.12km2 in 1990 to 282.82km$^2$ in 2020. The transitioning of the different Forest Canopy Densities from one category to another was also captured in this study. For instance between 2005 and 2020, about 37 km² changed from low density (LD) to no forest (NF). The accuracy assessment shows that the image classification is good in the sense that the Overall Accuracy figures are 69% (1990), 84% (2005) and 85% (2020). This forest modeling technique is very apt when it comes to the monitoring of forest cover dynamics, forest disturbance and ways of mitigating them.***

**Key words:** Geographic Information System, Remote sensing, Forest changes, Landsat, FCD, classification, anthropogenic and urbanization.

## INTRODUCTION

Consequent upon a plethora of anthropogenic activities such as farming, industrialization, mining, urbanization etc., there has been massive depletion of the forest ecosystems. These activities over the years have exacerbated the problem of deforestation. The study of forest canopy density is very important when considered against the backdrop of its relationship with forest ecosystem, biodiversity and forest health status (Banerjee et al., 2014). Several conventional remote sensing methods such as image classification, segmentation and slicing have been deployed by different researchers. Apart from the classification method that utilizes spectral training data for quantitative analysis, some other methods have inherent computational drawbacks. Therefore, Forest Canopy Density model developed by International Tropical Timber Organization (ITTO) to evaluate canopy density has become very useful. It therefore, behooves on policy makers in forest management and sustainable biodiversity to put a lot of premium on the monitoring of forest cover density.

Mapping of a wide range of natural resources has become more feasible through the deployment of geospatial technologies. Remote sensing involves the acquisition of spatial information about an object, or a phenomenon through the analysis of data acquired by a device that is not necessarily in direct contact with the object or phenomenon under investigation. On the other hand, Geographic Information System (GIS) is a system that captures, stores, manipulates analyses, manages and presents geospatial data or information for end users.

Therefore, GIS has the capabilities to manipulate and analyze spatial and temporal data that can be used to map, monitor and identify driving forces and measure the intensity of land use/land cover transformation (Samanta and Pal, 2016). Remote sensing and GIS provides a more robust and timesaving option for estimating forest canopy density, than the conventional way of ground monitoring which can be tedious and time-consuming (Deka et al., 2012). It suffices therefore to state that the importance of forest canopy density (FCD) model in assessing forest phenology, forest health and other biophysical components of the forest ecosystem through remote sensing application cannot be overemphasized. There is strong relationship between forest fragmentation and FCD. This explains why this study focuses on the rate of forest fragmentation which decimates forest cover into patches. A number of studies on the forest changing dynamics suggested that land acquisition/colonization and land use activities lead to discrete spatial patterns in the forest landscape (Godar et al.,2014, Wang and Caldas, 2014) and patch distributions over time (Rosa et al., 2012). This study is aimed at estimating the spatio-temporal changes of forest land cover by FCD model between 1990-2020 using geospatial technologies.

## MATERIALS AND METHODS

### Study Area

Sakpoba Forest Reserve lies between latitudes 4° to 4° 30' N and longitudes 6° to 6° 5' E. It is bounded on the south by Delta State, on the East by Urhonigbe Forest Reserve. It is located in Orhionmwon Local Government Area, about 30 kilometres South-East of Benin City (Azeez et al., 2010). Some of the major villages located within and around the reserve are Ugo, Ikobi, Oben, Iguelaba and Amaladi in Area B.C 32/4, and UgbokoNiro, Iguere, Idunmwowina, Evbarhue, Idu, Evbueka, Iguomokhua, Ona, Abe, Igbakele, Adeyanba, Evbuosa in Area B.C 29. The Benins are the original landowners and still form 80% of the population living within and around the forest reserve. There are other ethnic groups such as Urhobo, Itsekiri and Esan (Azeez et al., 2010).

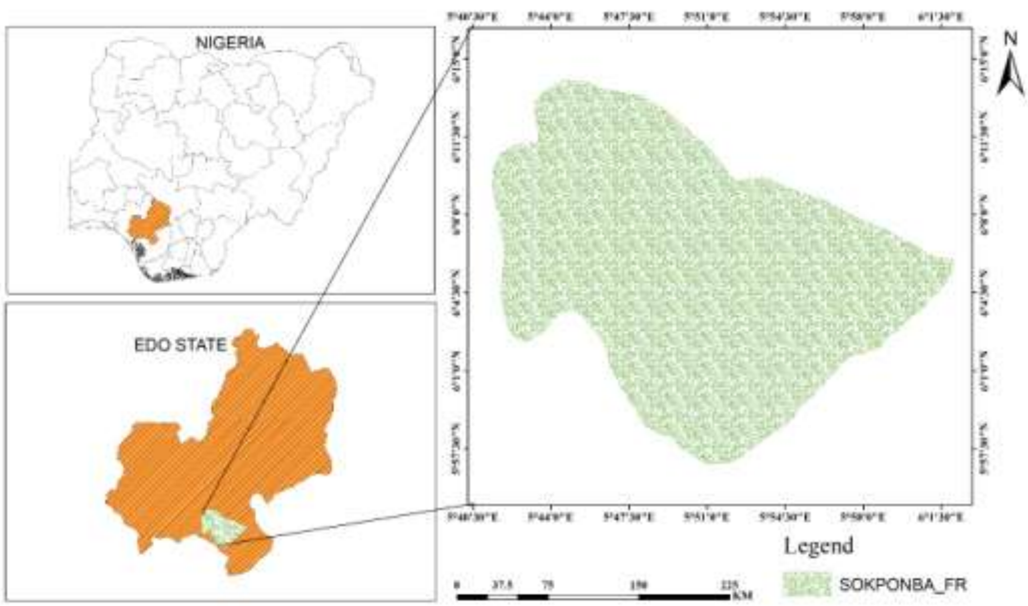


**Figure 1: Map of Sokpomba Forest Reserve**

### Data and software used

The Landsat images of years 1990, 2005 and 2020 downloaded from USGS Earth Explorer https://earthexplorer.usgs.gov) were used for the Forest Canopy Density (FCD) modeling The Google Earth Images of years 1990, 2005 and 2020 were used to aid the selection of training data for supervised classification The ground control points (GCP) used for the accuracy assessment of the classified imagery were collected during field visit to the study area The QGIS 3.12.0 software was used for atmospheric correction of Landsat imagery and accuracy assessment Are GIS 10.4 was used to create shape files and image classifications The calculation of FCD of the various years were carried out using Idrisi Selva software. It was also used for change detection analysıs and projection.

**Methods of calculating Forest Canopy Density (FCD)**

Images acquired by Landsat sensors are subject to distortions as a result of sensor solar atmospheric, and topographic effects. Image preprocessing attempts to minimize these effects to the extent desired for a particular application (Nicholas et al, 2017) The images to be used in this study were atmospherically corrected and converted to Top of Atmosphere (TOA) radiance using the equation 1 (Giannini *et al.*, 2015)

$$L\lambda = \left(\frac{(L_{MAX}\lambda - L_{MIN}\lambda)}{Q_{CAL}\lambda}\right) Q_{CAL} + L_{MIN}\lambda \text{ .......... (1)}$$

Where;

$L\lambda$ Is Spectral radiance at the sensor's aperture [W/ ($m^2$ sr μm)]

$Q_{CAL}$ is Quantized calibrated pixel value [DN]

$L_{MIN}$ $\lambda$ is Spectral at-sensor radiance that is scaled to $Q_{CAL}$MIN [W/($m^2$ sr μm)]

$L_{MAX}$ is Spectral at-sensor radiance that is scaled to Qcalmax [W/ (m 2 sr μm)].

The above expression does not consider the atmospheric effects, therefore the images were converted from radiance to reflectance measures, using equation below (Giannini *et al*, 2015).

$$\rho\lambda = \frac{(\pi * TOAr. * d^2)}{E_{SUN}\lambda . Cos\theta_{sz}} \text{ ........... (2)}$$

Where;

$\rho\lambda$ *is* Planetary TOA reflectance (unitless)

$\pi$ *is* mathematical constant approximately equal to 3.14159 (unitless)

$L\lambda$ *is* Spectral radiance at the sensors aperture [w/ ($m^2$ sr μm)]

$d^2$ *is* The earth-Sun distance (Astronomical unit)

$E_{SUN}$ *is* Mean exo-atmospheric solar irradiance [w/ ($m^2$ sr μm)].

$\theta_{SZ}$ is the solar zenith angle (degree). The cosine of this angle is equal to the sine of the sun elevation $\theta_{SE}$. That is, $\theta_{SZ}$ is cos (90- $\theta_{SE}$ )

**Calculation of Forest Canopy Density**

The forest canopy density CDI 1S one of the models for evaluation of forest canopy density Some researchers who used this model in their studies, concluded that FCD model can be a feasible and accurate approach to the estimation of forest crown canopy density (Deka *et al.*, 2013 Banergee *et al.*, 2014, Godinho *et al.*, 2016). The use of a low pass filter (3 x 3 or 5 x 5) can increase the accuracy of classification-average increment 5% (Pakkhesal et al, 2013)

FCD model is often calibrated from 1-100% and can be calculated using indices like Advanced Vegetation Index (AVI), Bare Soil Index (BSI or BI), Shadow Index (SI) and Thermal Index (TI)

Figure 2 shows the methodological flow chart of the study.

**Vegetation Indices used for the Calculation of FCD**

**Advance Vegetation Index (AVI):**

Sequel to NDVI limitation in highlighting the differential in canopy density, it has become imperative to improve it by using power degree of the infrared response. Advanced Vegetation Index (AVI) has high sensitivity for the calculation of forest density due to its normalization capacity to atmospheric effects (Saurabh and Arvind, 2018). AVI can be calculated using equation 3.

$AVI$ = {($B6$ +1) (65536−$B4$) ($B5$ −$B4$)] 1/3 (for OLI) .......... (3)

AVI = [(B4 +1)*(256-B3)*(B4-B3)] 1/3 (for ETM) ............ (4)

**Shadow Index (SI):**

The ambient temperature of the forest ecosystem is traceable to tree shadow inside the forest evaporation from the leaf morphology. Therefore younger trees tend to cast low shadow when compared to matured trees. It is calculated using equation 5 or 6 (Saurabh *et al.*, 2018).

$SI$ = {(65536−$B2$)*(65536-$B3$)*(65536-$B4$)} 1/3 (for OLI) ....... (5)

$SI$ = {(256−$B1$)*(256-$B2$)*(256-$B3$)} 1/3 (for ETM) ........(6)

**Bare Soil Index (BSI or BI):**

The bare soil index increases as the percentage bare soil exposure of ground increases. This index helps in separating the vegetation with a different background. BI utilizes the combination of the blue, red, near infrared and short wave infrared spectral bands to capture soil variations. This index is calculated using equation 7 or 8 (Saurabh *et al.*, 2018)

$BI = ((B6+B4) - (B5+B2\ (B6+B4) + (B5+B2)) *100+100$ (for OLI) …… (7)

$BI = ((B5+B3) - (B4+B1\ (B5+B3) + (B4+B1)) *100+100$ (for ETM) ……(8)

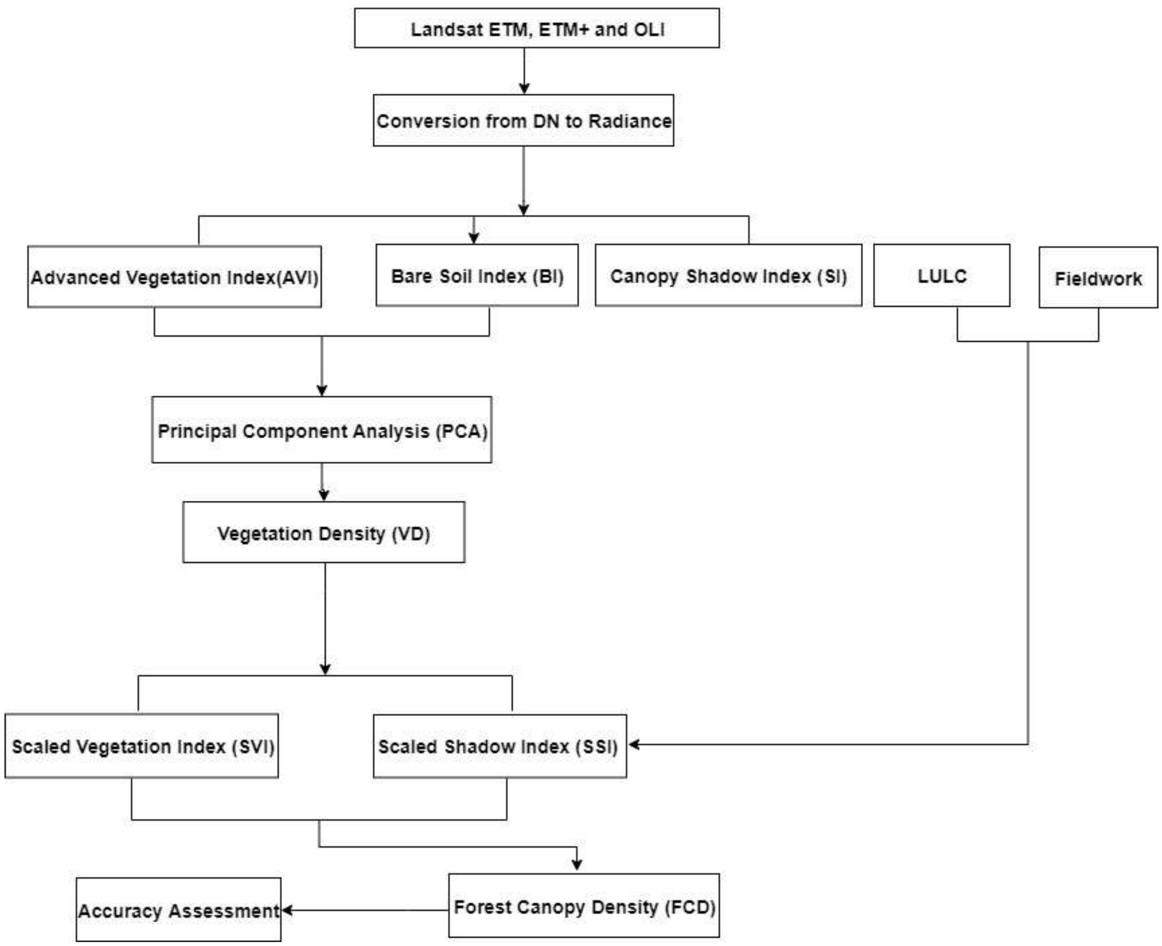


**Figure 2: Methodological flowchart.**

**Calculation of Forest Canopy Density**

Forest Canopy Density value was calculated in percentage for each pixel and it ranges from 0 to 100. One of the component indices for the calculation of FCD is the vegetation density (VD). It is derivable from the Principal Component Analysis (PCA) with AVI and BI as input parameters. VD value is rescaled from 0 to 100. Canopy shadow index (SI) is linearly transformed into Scaled Shadow Index (SSI), using the Fuzzy Membership Transformation algorithm. The input raster was transformed to 0 - 1 scale indicating the strength of membership in a dataset (Slady et al, 2016). The value of SSI is further rescaled from 0 to 100 percent (Jai, et al., 2015). Maximum SSI (100%) represents the highest possible shadow while the minimum represents the lowest possible shadow. It is the synthesis of the various indices discussed above that produces the FCD of the study area. It is scaled from 0 to 100 percent for easy interpretation. FCD is calculated using equation (9)

$FCD = \sqrt{VD * SSI + 1} - 1$ …………(9)

The Forest Cover Density (FCD) 1s classified into: No Forest (NF), Low forest density (LD) Moderate forest density (MD) and High forest density (HD). The classification is calibrated in percentages such as low forest density (<50%), middle forest density

(50-70%), and high forest density (>70%) according to Mohammad et al, (2020)

**The Markov Model**

This model is often used in monitoring, ecological modeling, simulation changes, trends of the LULC and to predict the amount of the land use change and the stability of future land development in the area of interest (Subedi *et al.,* 2013). Succinctly pat a Markov chain model describes the LULC change from one time to another in order to predict future change (D Behera et al., 2012). Equation (12) explains the calculation of the prediction of land use changes:

$$St\ (t, t+1) = Pij \times S\ (t) \ \ldots\ldots\ldots\ (10)$$

Where

S (t) 1s the system status at time of t

S (t +1) 1s the system status at time oft + 1,

Pij 1s the transition probability matrix in a state which is calculated as follows (Kumar et al, 2014)

**FCD Change Using Markov/CA-Markov Model**

CA-Markov model is quite instrumental in modelling land use changes and it can also be used to simulate and predict changes (Parsa *et al.* 2016) Spatio-temporal modeling and simulation of LULC change can be robustly analyzed using the combination of CA-Markov (Singh et al., 2015) The important properties of CA 1S that they demonstrate the spatial and dynamic process and that 1s why they have been broadly used in land use simulation (Ye et al., 2008). Besides, the state of each cell depends on the spatial and temporal state of its neighbors (Reddy et al., 2017). This explains why it 1s deployed in this study to simulate the dynamics of FCD and its prediction. Equation 11 shows the expression of CA model (Sang *et al.*, 2011).

$$\text{CA Model} = S\ (t, t+1) = f(S\ (t), N) \ \ldots\ldots\ldots\ (11)$$

Where

S (t + 1) is the system status at time of (t, t +1);

F(S (t), N) is functioned by the State probability of any time (N).

## RESULTS

In this study, the Forest Cover Density (FCD) is classified into: No-Forest (NF), Low Forest Density (LD), Middle Forest Density (MD) and High Forest Density (HD) depending on the percentages i.e. low forest density (<50%), middle forest density(50-70%), and high forest density (270%) (Mohammad *et al.*, 2020). Figures 6 -9 revealed that there has been a steady decrease in the forest cover density of the study area between 1990 and 2020. Statistics (Table 2) show that the No-Forest area increased from 1.07% in 1990 to 2.67% in 2005. It drastically increased to 11.52% in 2020. The increase in No-Forest (NF) area is indicative of the high level of deforestation evidenced in the forest ecosystem. Conversely, the High Forest Density decreased from 26.19% in 1990 to 23.87% in 2020. In Table 4 the canopy density changed from Low Density (LD) to High Density (HD) with about 21.08 km2 between 1990 and 2005. It decreased to 6.12km2 between 2005 and 2020. The sharp increase could be attributed to increased anthropogenic activities coupled with inabilities of stakeholders to properly manage the forest reserve. The change from High Density (HD) to Low Density (LD) amounted to 23.02km? Between 1990 and 2005. But between 2005 and 2020 it increased to 38.10 km$^2$. To add more value to this work. A FCD of the study for 2035 was predicted. The projected result (Table 2) shows that Non-Forest (NF) will increased from 11.52% to 14.25%. Low Forest Density (LD) decreased from 23.10% to 18.46°6. The Middle Forest Density (MD) increased from 41.51% to 44.50% while the High Forest Density (HD) increased from 23.87% to 22.80%.

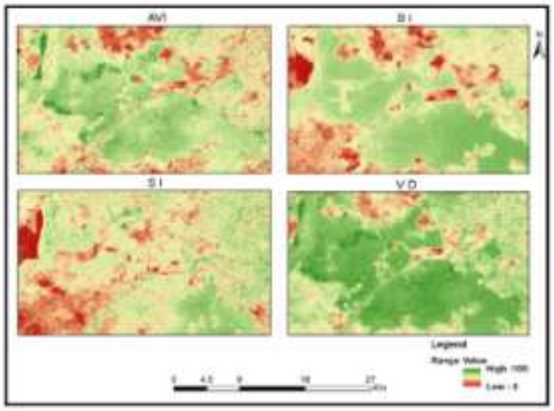


Figure 3: Vegetation indices (1990)

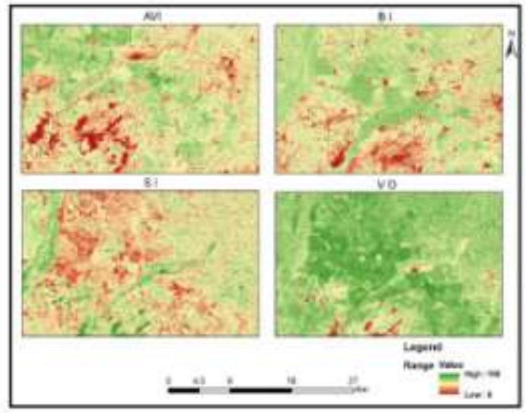


Figure 4: Vegetation indices (2005)

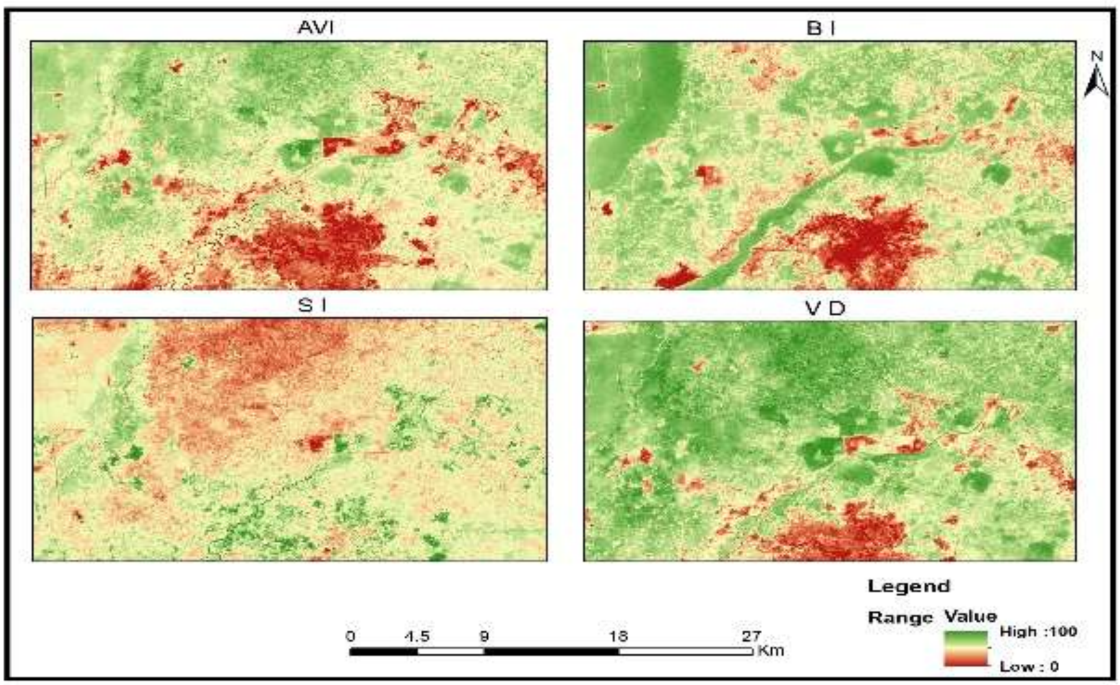


Figure 5: Vegetation indices (2020)

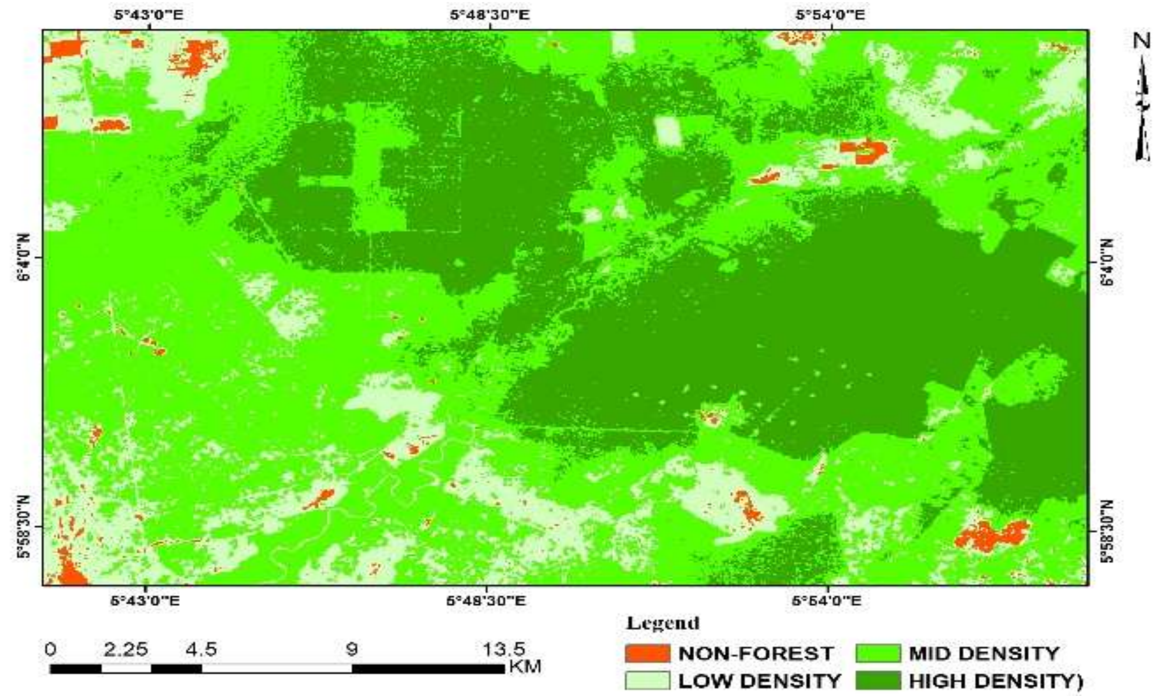


**Figure 6: FCD map of 1990**

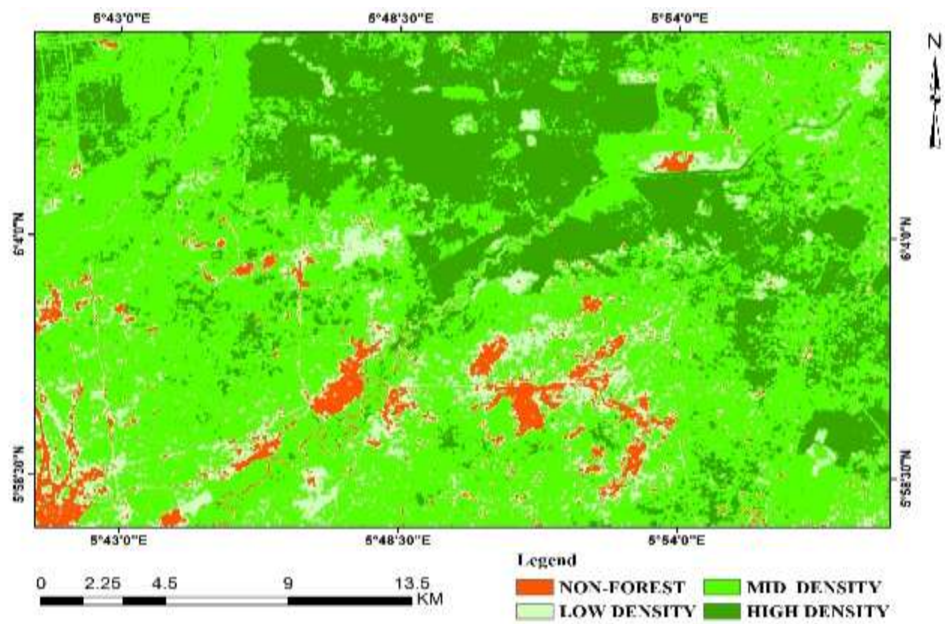


**Figure 7: FCD map of 2005**

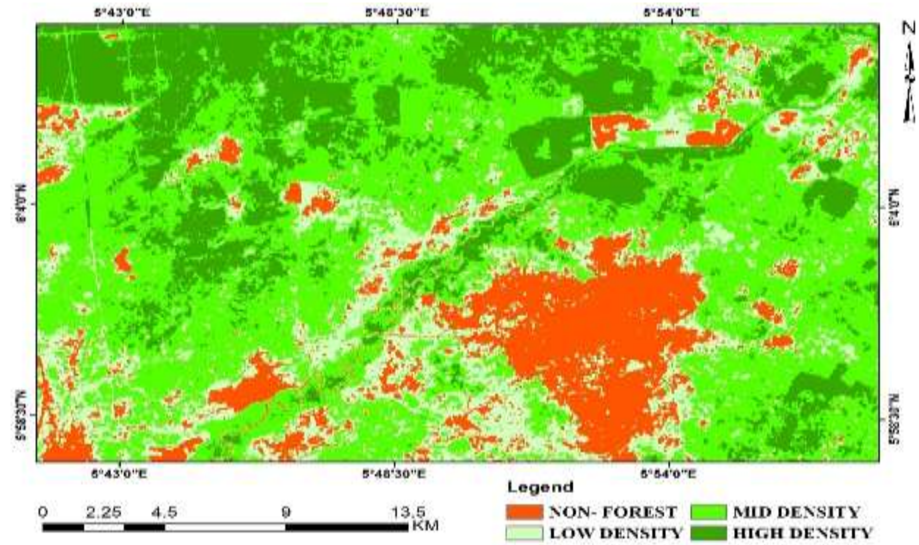


**Figure 8: FCD map of 2020**

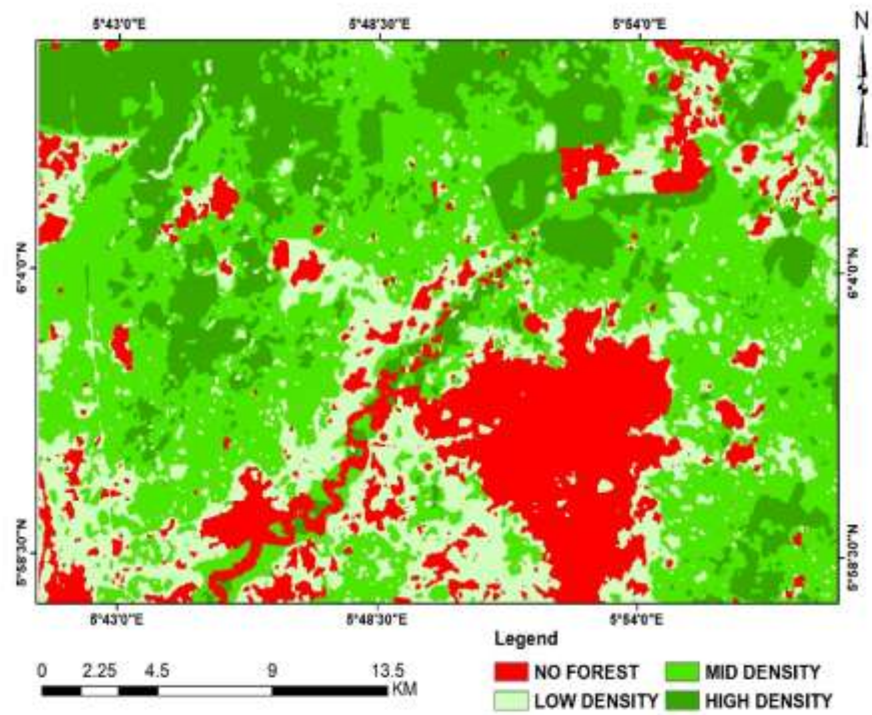


**Figure 9: FCD map of 2035**

**Table 1. Forest Canopy Density statistics from1990-2020 and 2035 predicted**

| FCD | 1990 | | 2005 | | 2020 | | 2035 | |
|---|---|---|---|---|---|---|---|---|
| | Area ($Km^2$) | Area (%) | Area ($Km^2$) | Area (%) | Area ($Km^2$) | Area (%) | Area ($Km^2$) | Area (%) |
| NF | 12.99 | 1.07 | 35.23 | 2.67 | 141.10 | 11.52 | 174.39 | 14.24 |
| LD | 171.12 | 13.97 | 119.25 | 9.09 | 282.82 | 23.10 | 226.16 | 18.46 |
| MD | 719.85 | 58.77 | 767.24 | 64.66 | 508.42 | 41.51 | 544.97 | 44.50 |
| HD | 320.82 | 26.19 | 303.05 | 23.58 | 292.39 | 23.87 | 279.26 | 22.80 |
| Total | 1224.78 | 100 | 1224.78 | 100 | 1224.78 | 100 | 1224.78 | 100 |

**Table 2: Forest Canopy Density statistics from 1990-2020 and 2035 (predicted)**

| FCD | 1990 | | 2005 | | 2020 | | 2035 | |
|---|---|---|---|---|---|---|---|---|
| | Area ($Km^2$) | Area (%) | Area ($Km^2$) | Area (%) | Area ($Km^2$) | Area (%) | Area ($Km^2$) | Area (%) |
| NF | 12.99 | 1.07 | 35.23 | 2.67 | 141.10 | 11.52 | 174.39 | 14.24 |
| LD | 171.12 | 13.97 | 119.25 | 9.09 | 282.82 | 23.10 | 226.16 | 18.46 |
| MD | 719.85 | 58.77 | 767.24 | 64.66 | 508.42 | 41.51 | 544.97 | 44.50 |
| HD | 320.82 | 26.19 | 303.05 | 23.58 | 292.39 | 23.87 | 279,26 | 22.80 |
| Total | 1224.78 | 100 | 1224.78 | 100 | 1224.78 | 100 | 1224.78 | 100 |

**Table 3: Forest Canopy Density change statistics**

| FCD | 1990-2005 | | 2005-2020 | | 2020-2035 | |
|---|---|---|---|---|---|---|
| | Δ ($Km^2$) | Δ (%) | Δ ($Km^2$) | Δ (%) | Δ ($Km^2$) | Δ (%) |
| NF | 22.24 | 1.6 | 105.87 | 8.85 | 33.29 | 2.72 |
| LD | -51.84 | -4.88 | 163.57 | 14.01 | -56.66 | -4.64 |
| MD | 47.39 | 5.89 | -258.82 | -23.15 | 36.55 | 2.99 |
| HD | --17.77 | -2-61 | -10.66 | 0.29 | -13.13 | -1.07 |

**Table 4: Forest Canopy Density change from 1990-2020 ($Km^2$)**

| Change Categories | 1990 - 2005 | 2005 - 2020 |
|---|---|---|
| Low Density to Non- Forest | 13.29 | 31.95 |
| Medium Density to Non-Forest | 10.47 | 66.66 |
| High Density to Non-Forest | 4.72 | 4.36 |
| Non-Forest to Low Density | 1.96 | 10.50 |
| Medium Density To Low Density | 50.21 | 131.85 |
| High Density to Low Density | 27.98 | 18.36 |
| Non-Forest to Medium Density | 5.61 | 4.31 |
| Low Density to Medium Density | 105.60 | 36.07 |
| High Density to Medium Density | 152.50 | 145.22 |
| Non-Forest to High Density | 1.22 | 0.60 |
| Low Density to High Density | 21.08 | 6.12 |
| Medium Density to High Density | 130.97 | 176.28 |

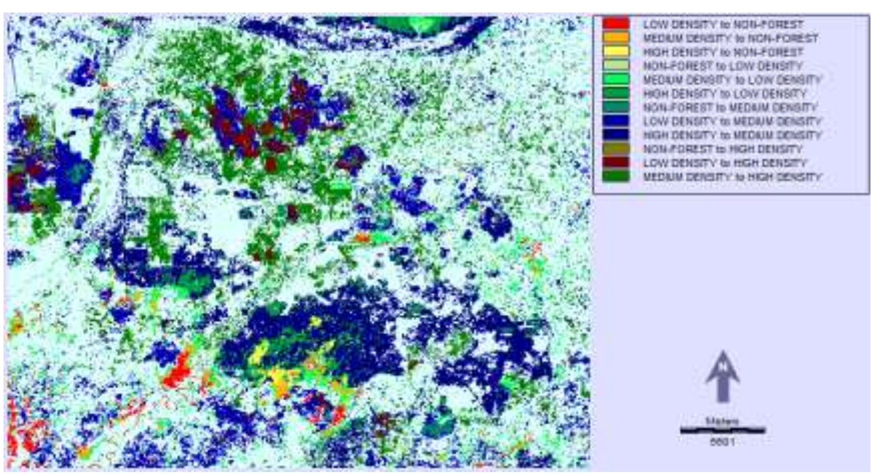


**Figure 10: FCD change map (1990 – 2005)**

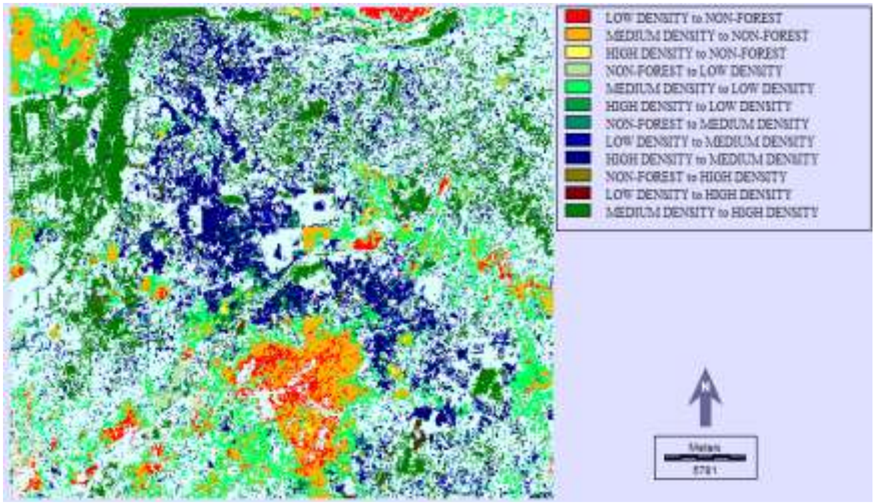


**Figure 11: Change map between 2005 and 2020**

**Table 5: Error Matrix of Forest Canopy Density**

| Class Name | 1990<br>Pa, Ua | 2005<br>Pa, Ua | 2020<br>Pa, Ua |
|---|---|---|---|
| No-Forest | 88,80 | 80,80 | 79,80 |
| Low Density | 83,83 | 83,88 | 93,87 |
| Middle Density | 78,75 | 83.71 | 92,85 |
| High Density | 70,78 | 88,93 | 47,90 |
| Kappa Coefficient | 0.77 | 0.78 | 0.76 |
| Overall Accuracy | 69% | 84% | 85.45% |

***Key:*** **Pa=Producer Accuracy; *Ua=User Accuracy*

## DISCUSSION

The obtained results of AVI as shown in Figure 2, show that the study area was well forested in 1990 when compared to years 2005 and 2020. The gradual reduction in AVI is an indication that the forest reserve was being depleted at an alarming rate. Looking at the Bare Soil Index (BI) map (Fig. 2), as the AVI was decreasing over time, the BI was increasing. This explains the fact that consequent upon uncontrolled anthropogenic activities, the bare soil was more and more exposed since the index helps to spectrally distinguish bare soil from other land covers. The Shadow Index (SI) helps in showing the shadow cast by trees in the forest. The taller the trees, the longer the shadow cast. In 1990, the SI map (Fig. 2) reveals that there are taller trees at the southern part of the study area. The index reduced drastically in the year 2020. By way of comparison, Pakkhesal et al., 2013, used Landsat ETM+ images to classify crown canopy of Shafarud Area of Guilan Iran, with different density classes (bare, 5–25, 25–50, 52–75 and 75–100%). The results of the four different indicators of FCD (AVI, BI, SSI, TI) show percentage of canopy density for each pixel. While the accuracy assessment of this study (Table 5) puts the overall accuracy at 84% and Kappa coefficient at 0.78, the classification accuracy of Pakkhesal et al., 2013, showed that the FCD map results were close to ground reality with overall accuracy of 71% and Kappa coefficient of 0.61. These similarities in accuracy assessment results add credence to the robustness of the pixel-based classification approach that was adopted for this study.

## CONCLUSION

This study, utilized FCD model to examine the forest canopy density of the study area from 1990 to

2020 deploying biophysical parameters such as AVI, SI and BI. The forest canopy density of the study area has experienced serious depletion of in terms of forest cover as shown in Figures 5, 6 and 7. It was revealed that over the years, a lot of square kilometers of land formerly occupied by high density forests have transitioned into middle density forest. The methodology applied for this work has proven to be a veritable tool in the sustainable management of forest cover and the entire forest ecosystem by extension.

## REFERENCES

Azeez I.O, Ikponmwonba O. S. Labode Popoola and T.O. Amusa (2010). Land Use Activities among Forest Environments' Dwellers in Edo State, Nigeria: Implications For Livelihood And Sustainable Forest Management. *International Journal of Social Forestry (IJSF),* 3(2):164-187

Banerjee, K., Panda, S., Bandyopadhyay, J. and Jain, M.K. (2014) Forest Canopy Density Mapping Using Advance Geospatial Technique. *International Journal of Innovative Science, Engineering & Technology,* 1, 358-363.

Behera, D. Borate, M. Panda, S. N. and Behera, P.R; Roy, P.S. (2012). Modelling and analyzing the watershed dynamics using Cellular Automata (CA)- Markov model-A geo-information based approach. *Journal of Earth System Science,* 1011-1024.

Deka, J., Tripathi, O.P. and Khan, M.L. (2012) Implementation of Forest Canopy Density Model to Monitor Tropical Deforestation. *Journal of Indian Society of Remote Sensing*, 41, 469-475.

Giannini M. B., Belfiore O. R, Parente C and Santamaria R, (2015). Land Surface Temperature from Landsat 5 TM images: comparison of different methods using airborne thermal data. *(Journal of Engineering Science and Technology Review)* 8 (3): 83-90.

Godar, J., Gardner, T. A. Tizado E. J. and Pacheco, P. (2014). Actor-specific contributions to the deforestation slowdown in the Brazilian Amazon. *Proceedings of the National Academy of Sciences.* USA., 111: 15591-15596.

Godinho S., Guiomar N., Machado R., Santos P., Sà-Sousa P., Fernandes J.P., Neves N., Pinto-Correia T. (2016): Assessment of environment, land management, and spatial variables on recent changes in montado land cover in southern Portugal. *Agroforestry Systems,* 90: 177-192

Jai, K., Paras, T. , and Krishna, A. P. (2015). "Forest canopy density and ASTER DEM based study for dense forest investigation using remote sensing and GIS techniques around East Singhbhum in Jharkhand, India," *International Journal of Advanced Remote Sensing and GIS,* pp. 1026-1032..

Kumar, S.; Radhakrishman, N., and Mathew, S. (2014). Land use change modelling using a Markov model and remote sensing. *Geomatics Natural Hazards and Risk*, 5: 145-156

Muhammed A. F., Anggieani L. S., Ranggas D. P., Kuswantoro M.(2020). Application of Forest Canopy Density (FCD) Model for the Hotspot Monitoring of Crown Fire in Tebo, Jambi Province. *Journal Geograft Lingkungan Tropik,* 4 (1), 59-67

Nicholas E. Young, Ryan S. Anderson, Stephen M, Chignell, Anthony G. Vorster, Rick Lawrence, and Paul H. Evangelista (2017). A survival guide to Landsat preprocessing. *Ecology,* 98(4): 920-932

Pakkhesal E., Bonyad A.E, (2013): Classification and delineating natural forest canopy density using FCD Model (case study: Shafarud area of Guilan). *Iranian Journal of Forest and Poplar Research*, 21: 99-114

Parsa, V.A, Yavari, A., and Nejadi, A. (2016). Spatio-temporal analysis of land use/land cover pattern changes in Arasbaran Biosphere Reserve: Iran. Model. *Modeling Earth Systems and Environment,* 2, 1-13.

Reddy, C.S., Singh, S., Dadhwal, V.K., Jha, C.S., Rao, N.R. and Diwakar, P.G. (2017. Predictive modelling of the spatial pattern of past and future forest cover changes in India. *Journal of Earth System Science* 126, 8-15.

Rosa, I.M.D., C. Souza Jr. and R.M. Ewers, (2012). Changes in size of deforested patches in the Brazilian Amazon. *Conservation Biology*, 26: 932-937.

Samanta, S. and Pal, D.K. (2016) Change Detection of Land Use and Land Cover over a Period of 20 Years in Papua New Guinea. *Natural Science*, 8, 138-151. http://dx.doi.org/10.4236/ns.2016.83017

Sang, L.; Zhang, C.; Yang, J.; Zhu, D. and Yun, W. ( 2011). Simulation of land use spatial pattern of towns and villages based on CA-Markov model. Math. Comput. Model .*Mathematical and Computer Modelling*, , 54, 938-943

Saurabh K. G and Arvind C. P. (2018). Forest canopy density and fragmentation analysis for evaluating spatio-temporal status of forest in the hazaribagh wild life sanctuary, Jharkhand (India). *Research Journal of Environmental Sciences*,12: 198-212

Singh, S.K., Mustak, S.; Srivastava, P.K.; Szabo, S.; Islam, T. Predicting spatial and decadal LULC changes through cellular automata Markov chain models using earth observation datasets and geo-information. *Environmental Processes*, 2, 61-78

Slady Akike and Sailesh Samanta (2016). Land Use/Land Cover and Forest Canopy Density Monitoring of Wafi-Golpu Project Area, Papua New Guinea

Subedi, P.; Subedi, K,; and Thapa, B. (2013). Application of a hybrid cellular automaton-Markov (CA-Markov) Model in land-use change prediction: A case study of Saddle Creek Drainage Basin, Florida. *Applied Ecology and Environmental Sciences*,1: 126-132

Wang, C. and M.M. Caldas, (2014). Fragmentation patterns in land reform settlements in the Brazilian Amazon. *Society and Natural Resources International Journal*, 27: 742-758.

Ye, B. and Bai, Z. (2008). Simulating land use/cover changes of Nenjiang. County based on CA-Markov model. *Computer and Computing Technologies in Agriculture*,1: 321-329.